J Therm Anal Calorim (2012) 109:1039–1047
DOI 10.1007/s10973-011-1882-1

# Thermal degradation and evolved gas analysis of thiourea-formaldehyde resin (TFR) during pyrolysis and combustion

**Tansir Ahamad · Saad M. Alshehri**

Received: 20 March 2011 / Accepted: 22 August 2011 / Published online: 10 September 2011


**Abstract** Thiourea formaldehyde resin (TFR) has been synthesized by condensation of thiourea and formaldehyde in acidic medium and its thermal degradation has been investigated using TG-FTIR-MS technique during pyrolysis and combustion. The results revealed that the thermal decomposition of TFR occurs in three steps assigned to drying of the sample, fast thermal decomposition of polymers, and further cracking. The similar TG and DTG characteristics were found for the first two stages during pyrolysis and combustion. The combustion process was almost finished at 680 °C, while during pyrolysis a total mass loss of 93 wt% is found at 950 °C. The release of volatile products during pyrolysis are $NH_3$, $CS_2$, CO, HCN, HNCS, and $NH_2CN$. The main products in the second stage are $NH_3$ $CO_2$, $CS_2$, $SO_2$, and $H_2O$ during combustion. In the next stage, the combustion products mentioned above keep on increasing, but some new volatiles such as HCN, COS etc., are identified. Among the above volatiles, $CO_2$ is the dominant gaseous product in the whole combustion process. It is found that the thermal degradation during pyrolysis of TFR produced more hazardous gases like HCN, $NH_3$, and CO when compared with combustion in similar conditions.

**Keywords** Thiourea-formaldehyde resin · Polymer · Thermal degradation · TG-FTIR-MS

T. Ahamad · S. M. Alshehri (✉)
Department of Chemistry, King Saud University, P.O. Box 2455, Riyadh 11451, Kingdom of Saudi Arabia
e-mail: alshehri@ksu.edu.sa

## Introduction

Amino resins are often used to modify the properties of other materials [1, 2]. These resins are used during the processing of new products such as textile fabrics to impart permanent press characteristics; automobile tires to improve the bonding of rubber to tire cord; paper to improve the tear strength, especially of wet paper; and alkyds and acrylics to improve their cure. The ability of formaldehyde to form resinous polymers had been observed by chemists in the second half of the nineteenth century. In 1918 Hans John prepared polymeric resins by reacting urea with formaldehyde. The reaction was studied more fully by Pollak and Ripper in an unsuccessful attempt to produce an organic glass during the period 1920–1924. At the end of this period E. C. Rossiter suggested that thiourea condensed with formaldehyde resulting in the production of thiourea formaldehyde resin (TFR) [3]. Today these resins are used extensively for molding powders, adhesives and textile and paper finishing while the related melamine–formaldehyde materials are also used in decorative laminates. Formaldehyde based polymers are widely used as construction materials in the field of wood, domestic buildings, etc. [4, 5]. However, formaldehydes based polymers and resins have been used as coating materials in various paint industries [6, 7]. Amino-formaldehyde resins are also used for molding products, such as electrical devices, jar caps, buttons, and dinnerware, and in the production of bangles [8, 9]. Formaldehyde based polymers are easy to burn at about 300 °C [10]. During the combustion of these polymers, a large amount of toxic fume is released out. The asphalt smoke is composed of small carbon particles and other combustible volatiles, which are much hazard to people. The smoke harm often outpaces the fire itself. Eighty-five percent of deaths in a

fire are due to inhaling toxic smoke [11]. Therefore, it is of primary importance to study the flammability of these polymers. The aim of this study is to investigate the thermal decomposition of TFR and its polymer metal complexes using TG-FTIR-MS.

## Experimental

### Materials

Thiourea, formaldehyde (37% aqueous solution), and acetic acid were used without further purification. TFR has been synthesized according to Scheme 1. In a 250 mL three-necked round-bottomed flask, 15.2 g (0.2 mol) of thiourea was dissolved in 20 mL distilled water, then 15 mL (0.2 mol) of a 37% aqueous solution of formaldehyde was added, and the pH was adjusted to 4 with acetic acid. The mixture was stirred magnetically and the temperature increase up to 90 °C and maintained for 6 h. The resulting colorless viscous product was washed with diluted NaOH solution, distilled water, ethanol, and acetone and dried in a vacuum oven under reduced pressure at 60 °C for 10 h [12]. After being dried in an oven at 105 °C for 3 h, the original materials were crushed and pulverized into a size of lower than 0.2 mm for further analysis.

$^1$H-NMR (300 MHz, DMSO,$\delta$) 6.30-6.80(N$\underline{H}$); 4.02–4.25 (=N-C$\underline{H}_2$-N), 3.65–3.75 (O-C$\underline{H}_2$-N); 3.5–3.75 (-NH-C$\underline{H}_2$-N); FTIR (KBr pallets)$\nu_{(max)}$ (cm$^{-1}$): 3500–3200, 2940–2850, 1680, 1470, 1440, 755. Anal. Calcd: C, 31.85; H, 5.75; N, 14.77; S, 28.31 Found: C, 31.82; H, 5.77; N, 14.74; S, 28.32.

### Method

The TG-FTIR-MS experiments were performed using simultaneous thermogravimetry (STD 600 TA Instrument) coupled with FTIR (Bruker Tensor 27) and mass spectrometry (Thermo). Helium was used as carrier gas with a flow rate of 100 mL min$^{-1}$ during pyrolysis and on the other hand oxygen was used as oxidant during combustion at similar flow rate. The coupling system between TG, FTIR, and MS was heated at 200 °C to prevent condensation of evolved gases and the heating rate of the furnace was 10, 20, 30, and 50 °C min$^{-1}$. It was found that the intensity of the thermal decomposition and the emission of gaseous products were slowed down at lower heating rates, but the similar components of gaseous products were observed. So the heating rate of 30 °C min$^{-1}$ was adopted for thermal decomposition of TFR. During TG/FTIR experiments, spectral data are repeatedly collected in the form of interferograms and then processed to build up a Grame Schmidt reconstruction, each point of which corresponds to the total IR absorbance of the evolved components in the range of 4000–500 cm$^{-1}$.

The mass spectrometer was operated at 70 eV electron energy. As such the *m/z* was carried out from 1 to 100 amu to determine which *m/z* has to be followed during the TG experiments. The ion curves close to the noise level were omitted. Finally, only the intensities of 22 selected ions (*m/z* = 12, 14, 15, 16, 17, 18, 20, 26, 27, 28, 30, 31, 32, 40, 42, 43, 44, 59, 60, 64, 76 and 78) were monitored with the thermogravimetric parameters.

## Results and discussion

Coupling a TG instrument with evolved gas analyzers, such as FTIR and a mass spectrometer, produces a very powerful analytical tool that gives information from the thermal balance as well as information from the spectrometers simultaneously and gives important information regarding the nature and mechanism of thermal decomposition [12]. The TG-FTIR-MS system has suitable interfaces to carry the gaseous decomposition products from the TG furnace to the detection system of FTIR and MS spectrometers, i.e., the method consists of carrying the evolving volatile products out of the furnace directly into the FTIR gas cell and MS where the gases are analyzed.

### TG/DTG of TFR during pyrolysis and combustion

The TG and DTG curves at a heating rate of 30 °C min$^{-1}$ are shown in Figs. 1 and 2. The pyrolysis process can be divided into three stages: drying stage (<190 °C), main pyrolysis stage (190–380 °C), and carbonization stage (>400 °C). The first mass loss between 100 and 200 °C corresponds to the vaporization of moisture and desorption

**Scheme 1** Synthetic route of thiourea formaldehyde resin

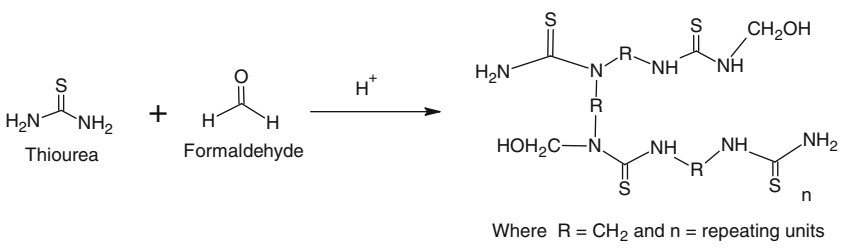

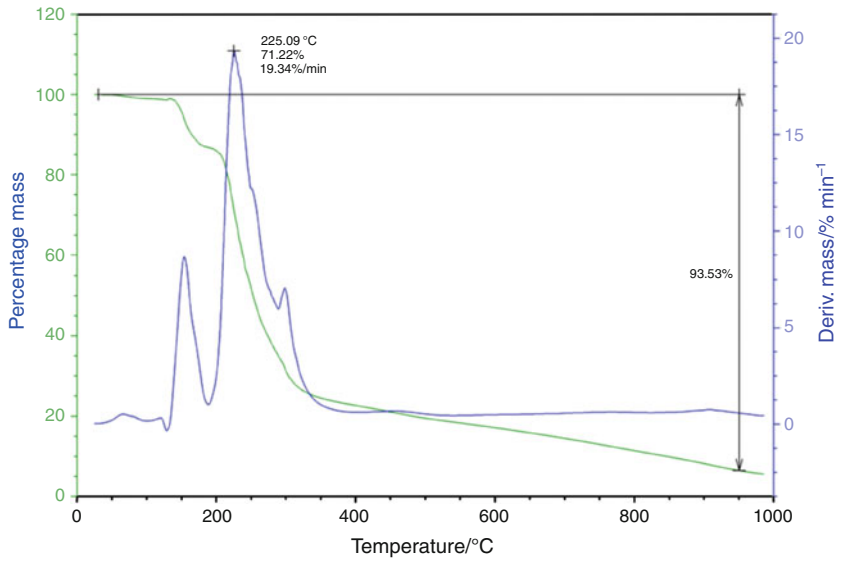


**Fig. 1** Tg/DTG of TFR during pyrolysis

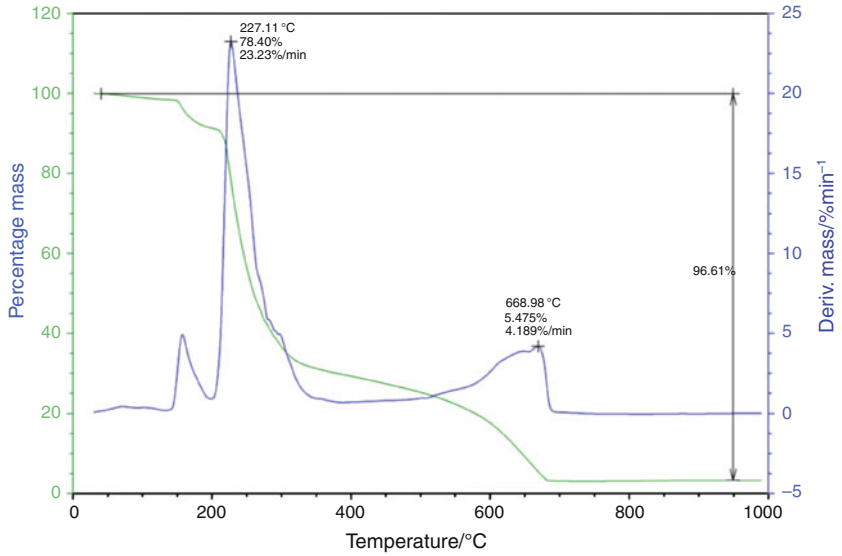


**Fig. 2** Tg/DTG of TFR during combustion

of water. The most significant mass loss (about 73% of the total mass of the sample) appears between 200 and 320 °C. There are two peaks of the DTG curve (mass loss rate) in this stage: the maximum mass loss rate occurred at 225 °C (19.34% $min^{-1}$), while the temperature at secondary peak is 298 °C (7.0495 $min^{-1}$). The last stage in TFR pyrolysis is further cracking process of the residues in a wide temperature range, from 370 °C to the end of this experiment (950 °C); about 20% mass of the total mass loss at a lower rate in this stage, and the total mass loss of 93.58.% mass was discovered at 950 °C during pyrolysis.

As seen from Fig. 2, at low temperature combustion of TFR shows similar thermogram as pyrolysis and shows about 68% mass of the total mass lost between 200 and 330 °C. The complete combustion of solid product finished quickly around 680 °C, which is quite different from the pyrolysis process. The combustion of the TFR polymer almost finishes after the mass loss peak between 400 and 680 °C, and about 29% mass of the original sample mass lost in this stage. The total mass loss of 96.61% mass is discovered at 950 °C in TFR combustion. There are no other solid products except ash content for TFR combustion at high temperature in oxidizing atmosphere. The comprehensive analysis for combustion and pyrolysis shows that almost all the solid products generated from TFR polymer pyrolysis can be burnt at high temperature, and 680 °C is enough for complete combustion of this polymeric resin. It is indicated that the characteristics of TFR combustion are quite different from the pyrolysis at high temperature.

**Table 1** Kinetic parameters (activation energy and Arrhenius pre-exponential factors) and coefficient of determination for the thermal degradation of TFR

| Temperature stage | Activation energy/J $mol^{-1}$ | Pre-exponential factor | $R^2$ |
|---|---|---|---|
| Pyrolysis at second stage | $6.73 \times 10^{-4}$ | 4.64E+002 | 0.954 |
| Combustion at second stage | $6.25 \times 10^{-4}$ | 3.01E+001 | 0.973 |
| Combustion at third stage | $1.37 \times 10^{-5}$ | 1.61E+003 | 0.942 |

## Pyrolysis and combustion kinetics

The first order reaction based Arrhenius theory is commonly assumed in the kinetic analysis during combustion and pyrolysis [13]

$$k = A\exp\left(-\frac{E}{RT}\right) \tag{1}$$

Where $k$ is constant of reaction rate, $T$ is thermodynamic temperature (K), $R$ is universal gas constant ($R = 8.314$ $Jmol^{-1}$ $K^{-1}$), $E$ is activation energy, and $A$ is a pre-exponential factor. The rate of decomposition may be expressed by:

$$\frac{d\alpha}{dt} = k(1-\alpha) \tag{2}$$

where $\alpha$ is mass loss fraction and defined as:

$$\alpha = \frac{m_0 - m_t}{m_0 - m_f}$$

where $m_0$ is the initial mass sample, $m_t$ is mass sample at $t$ time during thermal degradation, and $m_f$ is the final mass when experiment finished. Taking into account that temperature is a function of time and increases with constant heating rate $\beta$ the following expression derives:

$$T = \beta t + T_0 \tag{3}$$

Differentiating the above correlation, it derives:

$$dT = \beta dt$$

Equation 2 could be written as

$$\frac{d\alpha}{1-\alpha} = \frac{k}{\beta}dT \tag{4}$$

An integration function of above Eq. 4 is shown below

$$g(\alpha) = \int_0^{\alpha}\frac{d\alpha}{dt} = \frac{A}{\beta}\int_0^{t}\exp\left(-\frac{E}{RT}\right)dT \tag{5}$$

where

$$g(\alpha) = -\ln(1-\alpha)$$

Equation 5 is integrated by using Caots–Redfern method:

$$\ln\frac{g(\alpha)}{T^2} = \ln\left(\frac{AR}{\beta E}\left[1 - \frac{2RT}{E}\right]\right) - \frac{E}{RT} \tag{6}$$

where $g(\alpha)$ is the kinetic mechanism function in integral form.

As the term of $2RT/E$ can be neglected since it is much less than 1, Eq. 6 could be simplified as

$$\ln\frac{g(\alpha)}{T^2} = \ln\left(\frac{AR}{\beta E}\right) - \frac{E}{R}\frac{1}{T} \tag{7}$$

The term of $\ln(g(\alpha)/T^2)$ varies linearly with $1/T$ at a slope $-E/R$. Meanwhile, the intercept of the line with $y$-axis is related to the pre-exponential factor $A$. Both the activation energy $E$ and pre-exponential factor $A$ can be determined by the slope and intercept of the line and are presented in Table 1. It is observed that the activation energy of the first step during combustion is little more than that of pyrolysis in the first step while the activation energy in the second step for fixed carbon combustion is larger than the first step for volatile material combustion. It is concluded that the thermal decomposition of TFR polymer is accelerated by oxygen, which agrees well with the previous study of Font et al. [14].

## FTIR measurement

Gram-Schmidt reconstructs based on vector analysis of the acquired interferograms allows plots of the total evolved gases detected by the spectrometer to be generated (Fig. 3). The detector signal has been plotted as a function of sample temperature and qualitatively approximates DTA curves recorded during the TG experiments performed under different controlled conditions. It should be noted that the peaks in the Gram-Schmidt plot are shifted to higher temperatures than the corresponding DTG curve; this is due to the delay time between the gas generation and its detection in the FTIR equipment. The first and second peak during the combustion of TFR observed in the Gram-Schmidt is big, suggesting that the amount of the evolved gases in this stage is large and with high infrared extinction coefficients. In contrast, the third degradation stage seems to be composed of a small amount of evolved gases with low infrared extinction coefficients. The first peak observed in the Gram–Schimid plot during pyrolysis in small intensity suggests that the amount of evolved gas in this stage is low and with low infrared extinction coefficients. Figure 4 shows 3D FTIR

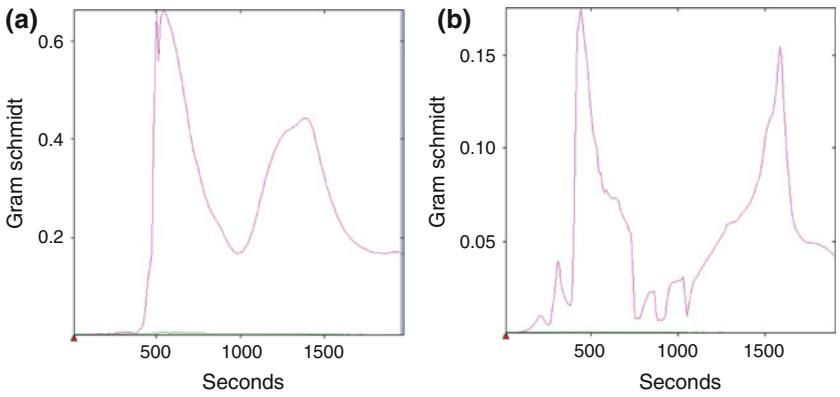


**Fig. 3** Gram-Schmidt plot during thermal degradation (**a**) combustion (**b**) pyrolysis

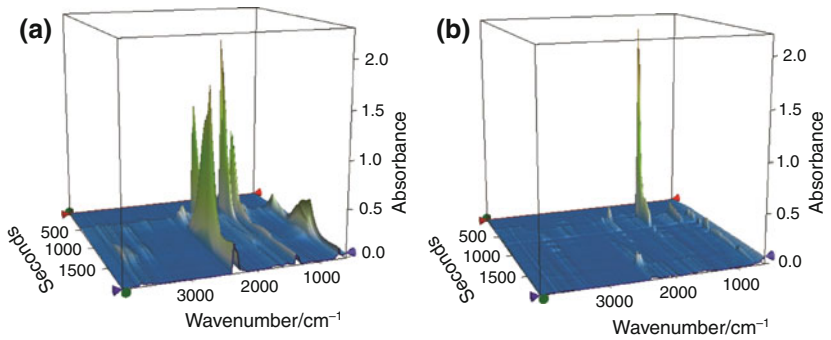


**Fig. 4** 3D FTIR plot during thermal degradation (**a**) combustion (**b**) pyrolysis

spectra for the gases produced from thermal degradation and Fig. 5a–c show the spectrograms at different temperature during pyrolysis and combustion of TFR at 250, 500, and 750 °C, respectively.

The main evolved products of the first degradation stage at 250 °C are identified as carbonyl sulfide (COS) and carbon disulfide ($CS_2$) with absorption bands at 2071 and 1539 $cm^{-1}$ during both pyrolysis and combustion [15]. Another one sharp band at 1375 $cm^{-1}$ is attributed to $SO_2$ during combustion while, this band is absent in the thermal degradation of TFR during pyrolysis. The TG-FTIR spectra during pyrolysis show two additional peaks at 946 and 930 $cm^{-1}$ that can be attributed to N–H stretching vibration of Ammonia [16].

The main gaseous products at 500 °C are $H_2S$, $CO_2$, $NH_3$, HCN, $CS_2$, and COS accompanied with a little methane ($CH_4$) during the pyrolysis of TFR. The presence of $NH_3$ and HCN as the main nitrogen-containing gases was confirmed by the appearance of two sharp bands at 966 and 714 $cm^{-1}$ respectively. It is also found that the emission of HCN and $NH_3$ as the main nitrogen-containing component with the increasing temperature, and the intensity of HCN and $NH_3$ emission reach their peak. The presence of $CO_2$ with very low intensity was confirmed by the appearance of very small bands at 2358 $cm^{-1}$ during the thermal degradation at 500 °C while during combustion the concentration of $CO_2$ is large and shows very strong band in the similar region.

Figure 5c shows the FTIR spectra of evolved gases during the thermal degradation at 750 °C. As observed the spectrum shows two very intense bands at 2250 and 2275 $cm^{-1}$ which was associated to cyanamide ($H_2N$–CN) and isocyanic acid (HN=C=O) during pyrolysis, and these two bands disappear during the combustion of TFR at 750 °C. Taking into account the above mentioned result it is possible to postulate that the main volatile product obtained are HCN, $NH_3$, HNCS, and $H_2S$ (during pyrolysis), and $CO_2$, $SO_2$, and COS (during combustion).

## MS measurement

The exact composition of the TFR degradation products was determined by thermogravimetry coupled to a Mass Spectrometer. The volatilization profiles, represented as Bar Graph of the fragments originating in the thermal degradation at 500 °C are shown in Fig. 6 during combustion and pyrolysis. The mass spectrum range recorded was from 1 to 100 *m/z*; no peaks were observed at higher *m/z* values. The release of carbon dioxide during this degradation stage was confirmed by a fragment at *m/z* 44, 28 16, 22, and 45 and it is also supported by FTIR data where carbon dioxide has been observed in all three stages, but it is much more pronounced in the second step of the degradation. The release of $SO_2$ during combustion at 500 °C was confirmed by the fragment at *m/z* 64, 48, 32, 16, and 78 and the presence of $H_2S$ in both type of thermal

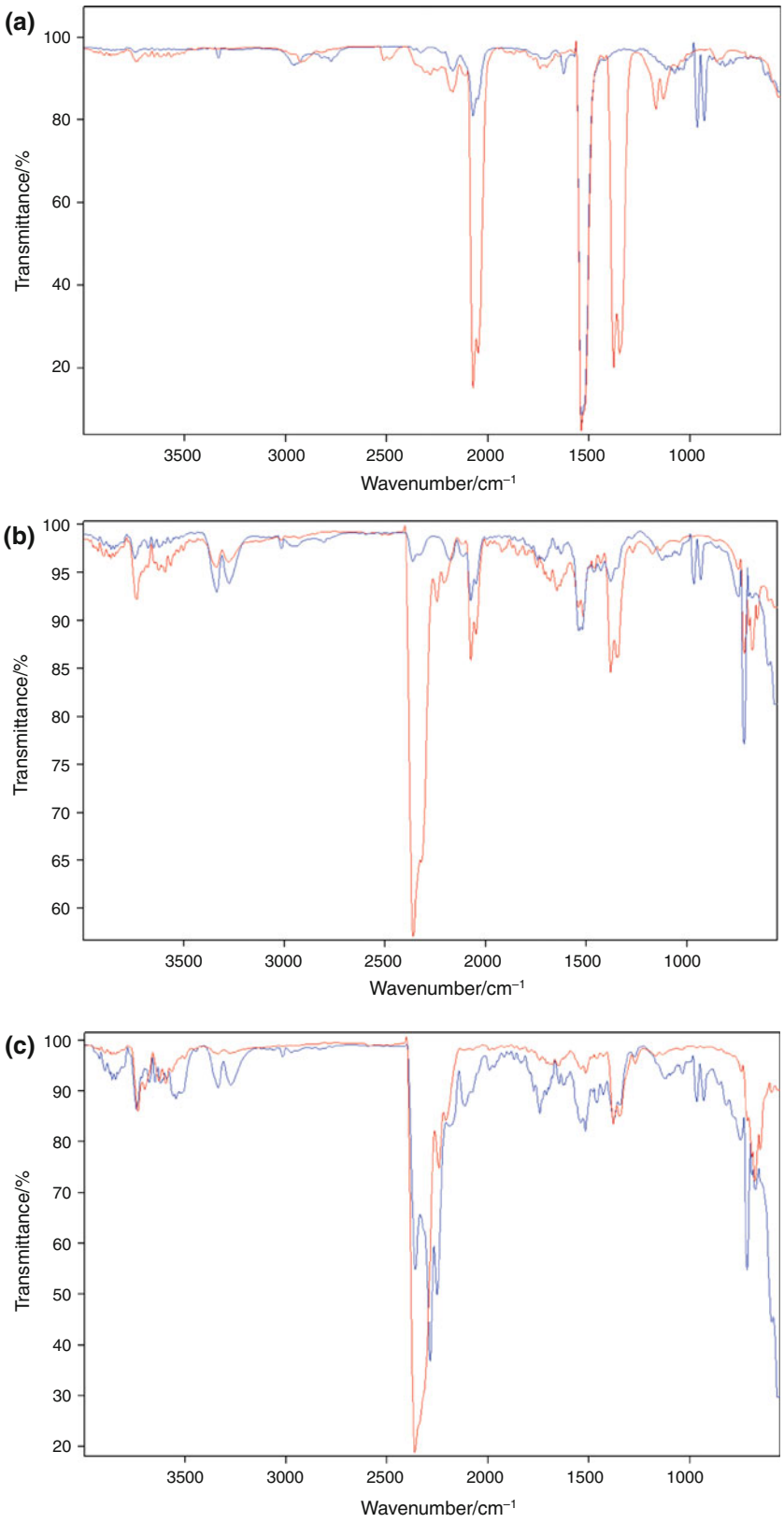


**Fig. 5** Spectrograms at different temperature during pyrolysis and combustion of TFR (**a**) at 250 °C (**b**) at 500 °C (**c**) at 750 °C (*Blue* for pyrolysis and *red* for combustion)

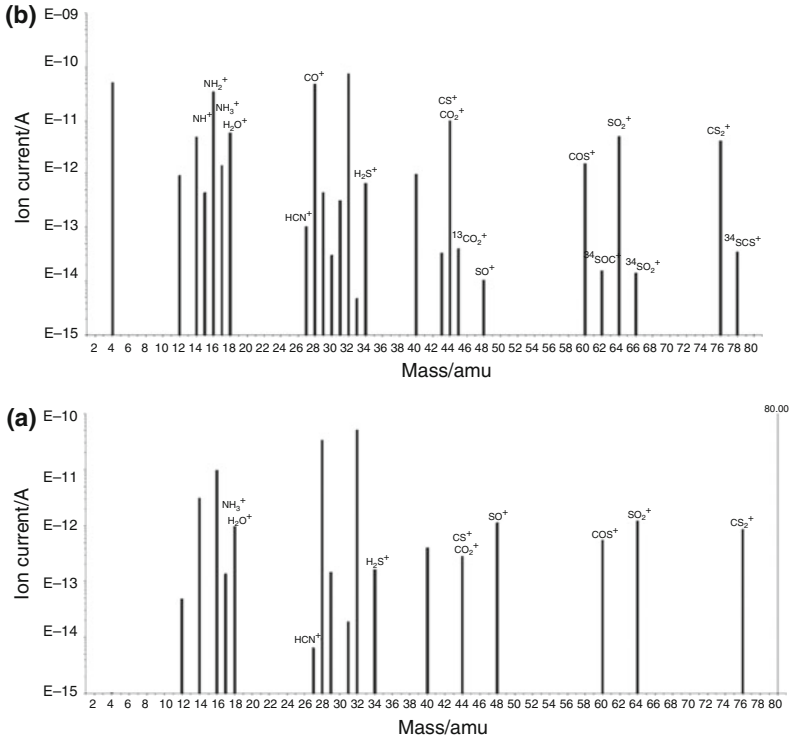


**Fig. 6** *Bar Graph* of the fragments originating in the thermal degradation at 500 °C (**a**) combustion (**b**) pyrolysis

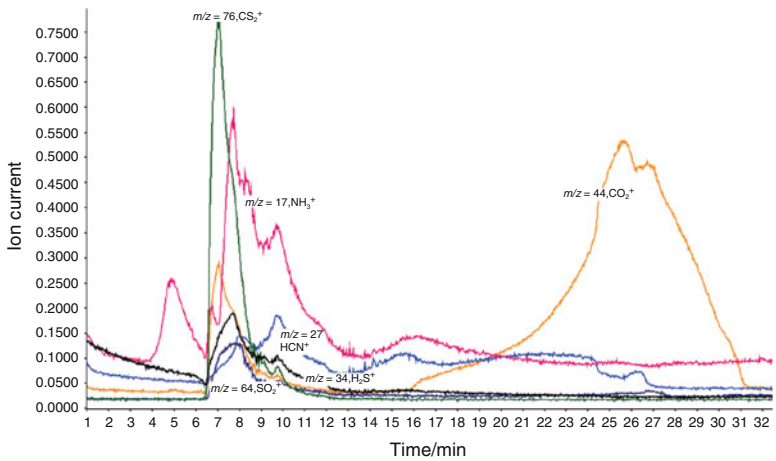


**Fig. 7** Single ion current curves during thermal degradation of TFR during pyrolysis

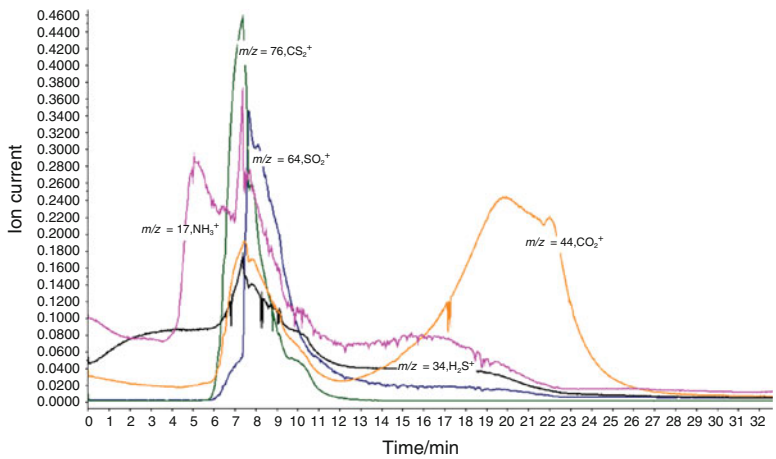


**Fig. 8** Single ion current curves during thermal degradation of TFR during combustion

degradation is supported by the fragments at *m/z* 34, 32, and 33 [20]. The releasing of water begins at 80 °C and show fragments at *m/z* 18 in the first and second degradation stage during pyrolysis and combustion of TFR.

The Single Ion Current during pyrolysis is shown in Fig. 7. The peaks at *m/z* 27 and 26 which appear with strong intensity in the second degradation step at 500 °C can be assigned to HCN [17]. The release of another gas during second stage degradation show fragment at *m/z* 76 and 78 due to the presence of $CS_2^+$ and $^{34}SCS^+$ ions during pyrolysis. These fragments start to appear in the second degradation step (from 195 °C) with low intensity, and continue to appear with high intensity in the second degradation step. The third stage degradation (polymer cracking) show some additional peaks at *m/z* 60, 32, and 28, which can be assigned to carbonyl sulfide (COS) fragments. Finally, $CH_4$ ($m/z = 16$) is mainly emitted after 675 °C due to the polymer cracking during pyrolysis [18]. The single ion current of the volatile species detected during the combustion of TFR are shown in Fig. 8. Carbon dioxide can be indentified ($m/z = 44$) in second and third degradation step. The *m/z* 64 ($SO_2$) is produced from the degradation of $CS_2$ carbon disulfide in the presence of oxygen in the second degradation step and is continuous with significant intensity in the third step.

$$CS_{2(g)} + 1.5O_{2(g)} \rightarrow SO_{2(g)} + COS_{(g)}$$

The comparison between the results obtained with the TG-FTIR and the TG-MS shows some differences. For all profiles, fewer fluctuations appears on the curves of FTIR than on TG-MS ones. This is probably due to the optical cell of FTIR, which tends to average the signals because of its volume. In addition, a shift of curves appears between these two techniques. It can be explained by the different residence time induced by the experimental devices. By regarding in detail each gaseous compound, we can note that for $H_2O$ and $CO_2$, the two profiles show same tendencies. Conversely, significant differences appear between the two analyses for CO and $CH_4$. With mass spectrometry, CO is followed with the fragment at *m/z* 28. As mentioned previously, the emission begins from 200 °C during combustion. Therefore, the emission between these two temperatures is likely due to other gaseous compounds such as HCN and $SO_2$. In addition, between 300 and 675 °C, CO production is overestimated by TG-MS. Some gases also appear on this temperature range and their ion fragmentation produces a fragment at $m/z = 28$. The same observation can be performed for $CH_4$. With FTIR, the release of $CH_4$ occurs only after 675 °C. With TG-MS, the fragment at *m/z* 15 shows an apparition of gases from 180 °C. The emission between 180 and 400 °C observed on TG-MS profiles can be attributed to other volatile products, which contribute to fragment at *m/z* 15. Thus, the FTIR analyses and the mass spectrometry have advantages and disadvantages. However, using information provided by each of them, it is possible to have an identification of the gases emitted by degradation of TFR during pyrolysis and combustion.

## Conclusions

The aim of this study was to compare the thermal degradation of thiourea- formaldehyde resin during pyrolysis and combustion. The activation energy of the first step during combustion was little more than pyrolysis. The result of TG-FTIR-MS revealed that the main volatile product obtained were HCN, $NH_3$, HNCS, and $H_2S$ (during pyrolysis), and $CO_2$, $SO_2$, and COS (during combustion). Some homogenous diatomic gases such as $H_2$ and $Cl_2$ etc., are released during the thermal decomposition, which are undetectable with FTIR. To follow all main gaseous products, further investigation was conducted using the coupling TG-MS. These two techniques are therefore complementary since they can refine the identification of gases.

## References

1. Pizzi A, Mittal KL. Handbook of adhesive technology. 2nd ed. New York: Marcel Dekker; 2003.
2. Hatjiissaak A, Papadopoulou E. Aminoplast resin of high performance for lignocellulosic materials. Greece: Chimar Hellas S.A.; 2007.
3. Brydson JA. Plastics materials, vol 5, 7th ed. London: Butterworth Heinemann; 2000. p. 668.
4. Kamola H. Focus on melamine. In: Proceedings of the International Surf. Conference. Amsterdam, Netherlands 2007; p. 89–93.
5. Hill G, Hedren AM, Meyers GF, Koutsky JA. Raman spectroscopy of urea–formaldehyde resins and model compounds. J Appl Polym Sci. 1984;29:2749–62.
6. Turnen M, Alvila L, Rainio L. Modification of phenol–formaldehyde resol resins by lignin, starch, and urea. J Appl Polym Sci. 2003;88:582–8.
7. Zmihorska GA. Phenol-formaldehyde resols modified by boric acid. Polimery (Warsaw). 2006;51:386–8.
8. Nalwa HS, Vasudevan P. Thermally stimulated depolarization effect in thiourea-formaldehyde condensate. Polymer. 1983;24:1197–202.
9. Ahamad T, Kumar V, Nishat N. Synthesis, characterization and antimicrobial activity of transition metal chelated thiourea-formaldehyde resin. Polym Int. 2006;55:1398–406.
10. Nishat N, Ahmad S. Rahisuddin, Ahamad T, Synthesis and characterization of antibacterial polychelates of urea–formaldehyde resin with Cr(III), Mn(II), Fe(III), Co(II), Ni(II), Cu(II), and Zn(II) metal ions. J Appl Polym Sci. 2006;100:928–36.
11. Tao X, Xiaoming H. A TG-FTIR investigation into smoke suppression mechanism of magnesium hydroxide in asphalt combustion process. J Anal Appl Pyrol. 2010;87(2):217–23.
12. Madarász J, Bombicz P, Matysa C, Reti F, Kiss G, Pokel G. Comparative evolved gas analytical and structural study on trans-

diammine-bis(nitrito)-palladium(II) and platinum(II) by TG/DTA-MS, TG-FTIR, and single crystal X-ray diffraction. Thermochim Acta. 2009;490:51–9.
13. Rath J, Staudinger G. Cracking reactions of tar from pyrolysis of spruce wood. Fuel. 2001;80:1379–89.
14. Font R, Fullana A, Conesa J. Kinetic models for the pyrolysis and combustion of two types of sewage sludge. J Anal Appl Pyrol. 2005;74:429–38.
15. NIST Chemistry Webbook standard reference database no. 69, Release (http://webbook.nist.gov/chemistry). EPA Vapor Phase Library 2005.
16. Pierson RH, Fletcher AN, Gantz ESC. Catalogue of infrared spectra for qualitative analysis of gases. Anal Chem. 1956;28:1218–39.
17. Birk M, Winnewisser M. The rotation-vibration spectrum of gaseous cyanamide (H2NCN). Chem Phys Lett 1986; 123:382–385.
18. Ma SB, Lu J, Gao JS. Study of the low temperature pyrolysis of PVC. Energy Fuel. 2002;16:338–42.